Biochemical Characterization of the L-Plastin−Actin Interaction Shows a Resemblance with That of α-Actinin and Allows a Distinction To Be Made between the Two Actin-Binding Domains of the Molecule†

M.-C. Lebart,* F. Hubert, C. Boiteau, S. Ventéo, C. Roustan, and Y. Benyamin

UMR 5539, Laboratoire de Motilité Cellulaire (EPHE), USTL, Bât.24, 4ème étage, cc 107, place E. Bataillon, 34095 Montpellier, France

Received June 16, 2003; Revised Manuscript Received December 1, 2003

ABSTRACT: Actin interaction with L-plastin, a plastin/fimbrins isoform of the α-actinin family of molecules, is poorly characterized, from the biochemical point of view. Besides, molecular modeling of the T-isoform has recently provided a complete model of interaction with filamentous actin [Volkmann, N., DeRosier, D., Matsudaira, P., and Hanein, D. (2001) *J. Cell Biol. 153*, 947−956]. In this study, we report that recombinant L-plastin binds actin in a manner that strongly resembles that of the α-actinin−actin interface. The similitudes concern the absence of specificity toward the actin isoform and the inhibition of the binding by phosphoinositides. Furthermore, the participation of actin peptides 112−125 and 360−372 in the interface together with an inhibition of the rate of pyrenyl F-actin depolymerization is in favor of a lateral binding of the plastin isoform along the filament axis and strenghtens the similitudes in the way L-plastin and α-actinin bind to actin. We have also investigated the functional aspect and the putative equivalence of the two actin-binding domains of L-plastin toward actin binding. We demonstrate for the first time that the two recombinant fragments, expressed as single domains, have different affinities for actin. We further analyzed the difference using chemical cross-linking and F-actin depolymerization experiments assayed by fluorescence and high-speed centrifugation. The results clearly demonstrate that the two actin-binding domains of plastin display different modes of interaction with the actin filament. We discuss these results in light of the model of actin interaction proposed for T-plastin.

L-Plastin (MW = 70 kDa) is an actin-bundling protein that belongs to the α-actinin family of proteins (*1*) and to the fimbrin subfamily, in which it exhibits functional conservation (*2*). *In vivo*, fimbrins (*3*) are found to be associated with unipolar filaments as in microvilli of epithelial cells, stereocilia of epididymis, and hair cell (*4*, *5*), and in adhesion sites, fimbrin is found at the cell−matrix interface where it was shown to interact with vimentin (*6*). All members of the fimbrin family share in commun two highly conserved actin-binding domains (ABDs),[1] forming the core of the molecule; the presence of a specific NH_2-terminal domain, eventually supporting calcium ("EF-hands" domains) and phosphorylation (only the L isoform) regulation, is also characteristic of this family (*7*−*10*). However, some new members of the family show particularities: *Tetrahymena* fimbrin, which is deprived of the N-terminal domain (*11*), and the *Arabidopsis thaliana* one bearing an additional sequence in its COOH-terminal sequence (*12*). L-Plastin was originally shown to be overexpressed in many cancers, particularly those associated with steroid hormone expression, i.e., ovarian, breast, and prostate carcinomas (*13*, *14*). This has recently led researchers to develop new therapeutic tools based on the L-plastin gene for slowing the progression of cancer *in vivo* (*15*, *16*). Under normal conditions, L-plastin expression is restricted to hematopoietic cells, whereas the other human isoform, T-plastin, is associated with all the other tissues.

In L-plastin, the core domain is formed by a tandem repetition of the two ABDs, the sequence of the first one (ABD1) being more homologous with the actin-binding domain of α-actinin (27 kDa) than the sequence of ABD2. More generally speaking, the degree of homology is higher between ABDs of different members of the fimbrin family (taken at the same position) than between the two ABDs of the same molecule. There is only limited biochemical data about the interaction of plastin with actin (*17*, *18*) and none about the actin-binding domains. These studies report that L-plastin bundling activity is inhibited by calcium in the micromolar range and that L-plastin binding to F-actin is isoform specific, since only the cytoplasmic β-isoform was shown to bind L-plastin.

New insight into actin binding was gained by the determination of the three-dimensional structure of part of the actin-binding domain of several members of the α-actinin

† This work was supported by Grant 9491 from the Association de Recherches contre le Cancer.

* To whom correspondence should be addressed. Telephone: (00 33) 4 67 14 38 89. Fax: (00 33) 4 67 14 49 27. E-mail: mclebart@univ-montp2.fr.

[1] Abbreviations: ABD, actin-binding domain; FITC, fluorescein isothiocyanate; I-AEDANS, *N*-(iodoacetyl)-*N*′-(8-sulfo-1-naphthyl)-ethylenediamine; EDC, 1-ethyl-3-[3-(dimethylamino)propyl]carbodiimide; EEDQ, *N*-(ethoxycarbonyl)-2-ethoxy-1,2-dihydroquinoline; ELISA, enzyme-linked immunosorbent assay; GST, glutathione *S*-transferase; IPTG, isopropyl thio-β-D-galactoside; SDS−PAGE, sodium dodecyl sulfate−polyacrylamide gel electrophoresis; PIP2, phosphatidylinositol 4,5-bisphosphate; PI, phosphatidylinositol; PBS, phosphate-buffered saline.

10.1021/bi030151p CCC: $27.50
Published on Web 02/10/2004

family, namely, ABD1 of T-plastin at 2.4 Å resolution (*19*), the C-terminal domain of human β-spectrin at 2.0 Å resolution (*20*), and the actin-binding region of the dystrophin homologue, utrophin, at 3.0 Å resolution (*21*, *22*). Sequence analysis and electronic microscopy have previously shown that each actin-binding domain resembles a tandem duplication of a calponin-like subdomain, termed "calponin homology domains" (CH). Plastin would thus contain four of these domains with unique particularity due the presence of a large inter-CH domain linker (*23*). An atomic model of T-plastin (segment 1−375) interaction with skeletal α-F-actin was deduced using electron cryomicroscopy and image analysis, placing ABD1 in a concave surface between two actin monomers along the long pitch helix of the microfilament (*24*, *25*). Sites of contact with plastin were proposed in actin subdomains 1 and 2. Recently, the first atomic model of complete actin−fimbrin cross-links was published (*26*). This study proposes a model for the whole fimbrin molecule based on crystallographic data (for ABD1) associated with molecular modeling for the ABD2 and the NH_2-terminal domains.

In the study presented here, we have investigated the interaction of expressed L-plastin with actin using fluorescence, solid phase assays, chemical cross-linking experiments, and high-speed centrifugation. We report biochemical similitudes of binding of L-plastin to the α-actinin−actin interface, which underline the lateral binding of the ABP along the filament axis. We also investigated the functional aspect and the equivalence of the two ABDs of L-plastin toward actin binding. We show that the two domains have different behaviors and demonstrate different modes of interacting with the actin filament.

EXPERIMENTAL PROCEDURES

Reagents. Biotin amidocaproate *N*-hydroxysuccinimide ester, alkaline phosphatase-labeled streptavidin, gelatin, its crude pancreatic digest, 5-bromo-4-chloro-3-indolyl phosphate (BCIP), nitro blue tetrazolium (NBT), glutathione−agarose beads, human thrombin, fluorescein isothiocyanate (FITC), EDC, NHS, and IAEDANS were purchased from Sigma. Ampholytes (pH ranges of 3−10 and 5−7) were from Fluka. Anti-rabbit immunoglobulins labeled with alkaline phosphatase were obtained from Valbiotech (Paris). Molecular mass markers for SDS−PAGE (between 14 and 97 kDa) were from Bio-Rad. PIP2, its derivatives, and monoclonal anti-β-actin (clone AC-15) were purchased from Sigma; glutathione was from Boerhinger. PD10 columns were from Pharmacia. All other chemicals were analytical-grade.

Proteins and Peptides. α-Actinin was prepared as previously reported (*27*).

Cytoplasmic β-actin was prepared from calf thymus using the following protocol. Ground tissue (100 g) was submitted to treatment with 3 × 150 mL of acetone. The crude acetone powder that was obtained (2−3 g) was then extracted in 20 volumes over the course of 20 min at 0 °C in buffer G [2 mM Tris-HCl, 0.1 mM $CaCl_2$, and 0.2 mM ATP (pH 7.8)]. After a first centrifugation (15 min at 35000*g*), the supernatant containing G-actin was clarified by ultracentrifugation (90 min at 100000*g*). The sample was filtered (0.45 μm) and then loaded on a Poros HQ/H anion exchanger column (Boehringer) using FPLC in 20 mM MOPS, 0.1 mM $CaCl_2$, and 1 mM DTT (pH 6.8), and actin was eluted at 28% of a buffer composed of 1 M NaCl, 0.1 mM $CaCl_2$, 1 mM DTT, and 20 mM Tris-HCl (pH 7.5). Fractions containing pure actin were pooled after being analyzed by 12.5% SDS−PAGE and dialyzed against buffer G. F-Actin was obtained after addition of 100 mM KCl, 2 mM $MgCl_2$, and 1 mM EGTA and ultracentrifugation (20 min at 300000*g*). The presence of different isoforms was checked using a two-dimensional gel (Bio-Rad). This method allowed us to recover 1.8 mg of actin made of 90% of the β-isoform from 1 g of total acetone powder.

Skeletal actin was isolated from acetone powder (*28*) and further purified when necessary as previously described (*29*). Monomeric actin complexed with magnesium (G−Mg) was obtained after dialysis against 1 mM EGTA, 0.1 mM $MgCl_2$, 0.2 mM ATP, and 10 mM MOPS (pH 7.2) (buffer A). Actin was labeled at Cys374 using 1.5-I-AEDANS (*30*), and pyrenyl F-actin was obtained as described in ref *31*.

Peptides encompassing residues 105−120, 112−125, 355−375, and 360−372 were synthesized on a solid phase support using the 9-fluorenylmethyloxycarbonyl-tertio-butyl system with a Milligen Pepsynthesizer TM 9050 (Milligen Bioresearch Division, Watford, U.K.). Each peptide was shown to be homogeneous using analytical HPLC and electrospray mass spectroscopy. Peptides 112−125, 360−372, and 355−375 were labeled at cysteine residue with 1.5-I-AEDANS according to the method described in ref *30*. Excess reagent was eliminated by sieving through a Bio Gel P2 column equilibrated with 100 mM NH_4HCO_3 (pH 8.3). Peptides 112−125 and 360−372 could be dansylated due to the addition of an extra Cys at the NH_2 extremity of the sequence.

L-Plastin was expressed after transformation of the GST−L-plastin fusion cDNA in the pGEX vector (gift of Dr. Arpin) in TG1 bacteria and grown at 37 °C in LB medium as a preculture (5 mL). This was used to innoculate a large culture (2 L) containing 100 μg/mL ampicillin. When the absorbance of the culture reached 0.6−0.9 at 595 nm, induction was performed with 1 mM IPTG and the cells were left to grow for 2 h at 37 °C. The cells were harvested by centrifugation, and the pellet was frozen. Cells were resuspended in lysing buffer [1 mM EDTA, 300 mM NaCl, 5 mM DTT, 20 mM Tris-HCl, and 0.2% NaN_3 (pH 8)] containing 100 μg/mL lysozyme. The mixture was sonicated (4 × 30 s) and centrifuged for 30 min at 100000*g*, and the supernatant was loaded on a glutathione−agarose column equilibrated in 300 mM NaCl, 1 mM EGTA, 1 mM DTT, 20 mM Hepes, and 0.02% NaN_3 (pH 7.2). After a washing step using 1 M NaCl, thrombin was added (10 units/mL of gel), and digestion was allowed to proceed for 1 h on a stirring wheel in 150 mM NaCl, 2 mM $CaCl_2$, and 50 mM Tris-HCl (pH 8). L-Plastin was recovered from the column, dialyzed against 100 mM KCl, 1 mM EGTA, and 20 mM MOPS (pH 7.2) (buffer B), and analyzed by 10% SDS−PAGE after Coomassie Blue staining as well as Western blotting (Figure 1a). GST was eluted using 10 mM glutathione in 50 mM Tris-HCl (pH 8.5). The capacity of expressed L-plastin to bind F-actin was previously reported using electron microscopy (*32*) and checked here in cosedimentation assays (not shown). L-Plastin (10−12 mg/L of culture) was used within 1 week. GST fusion constructs were generated by PCR cloning of L-plastin segments. cDNA regions encompassing residues 390−1208 (protein fragment 106−379) and 1215−1958

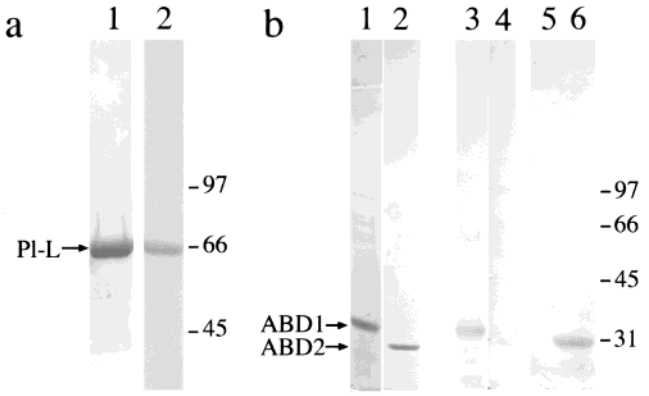

FIGURE 1: Purification of genetically expressed L-plastin and recombinant fragments. In panel a, SDS−PAGE (lane 1) and immunoblotting (lane 2) profiles of the fraction recovered from a glutathione−agarose column show that it is pure plastin (95%). Identification was achieved with the anti-NH_2-terminal antibodies (1 μg/mL, lane 2). In panel b, ABD1 and ABD2 fragments were submitted to SDS−PAGE (lanes 1 and 2) and transferred to nitrocellulose sheets (lanes 3−6); the membrane was revealed by the anti-ABD1 (1 μg/mL, lanes 3 and 4) and the anti-ABD2 (1 μg/mL, lanes 5 and 6), respectively. Note the specificity of each antibody reacting only with the related fragment. Molecular mass markers are given on the right.

(protein fragment 380−627) were amplified using synthetic oligonucleotide primers (Q-biogene) containing an extra nucleotide tail for a *Bam*HI or *Eco*RI restriction site at their 5′ or 3′ extremity, respectively, to allow cloning in pGEX-2T. Then, the procedure used to purify the actin-binding domains was identical to the one used for the L-plastin preparation. After thrombin digestion, the ABDs were dialyzed against 100 mM NaCl, 0.2 mM $CaCl_2$, and 20 mM MOPS (pH 7.1) (buffer C) and analyzed by 10% SDS−PAGE after Coomassie Blue staining as well as Western blotting (Figure 1b).

Plastin biotinylation was performed as described previously (*33*). Plastin labeling with FITC was carried out by incubating the reagent (protein/reagent molar ratio of 1/3) dissolved in *N*,*N*-dimethylformamide with the protein previously dialyzed against 100 mM $KHCO_3$ (pH 8.3). Excess reagent was removed using filtration over a PD-10 column equilibrated in buffer B supplemented with 300 mM NaCl.

Immunological Techniques. Three populations of antibodies directed against peptides chosen in the N-terminal domain and in ABD1 of the L-isoform as well as one chosen in ABD2 of T-plastin were elicited in New Zealand rabbits as previously described (*34*). As expected, the anti-ABD1 and anti-ABD2 antibodies were shown not to be specific for the fimbrin isoform in contrast to the NH_2-terminal specific antibody (*4*). Each antibody was purified by affinity chomatography on the related peptide as the immunoadsorbent (*35*).

An ELISA was used to test the affinity of the antibodies for the purified protein, to monitor the interaction between actin isoforms/peptides and biotinylated L-plastin (or ABD), and to investigate the effect of phosphoinositides on the actin−L-plastin interaction, as described by Lebart and colleagues (*27*). Actin, diluted in a 50 mM $NaHCO_3/Na_2CO_3$ mixture (pH 9.5), was immobilized on microtiter wells under nonpolymerizing conditions (300 ng/mL) for monomeric actin and at 50 μg/mL for filamentous actin. All incubations were followed by a washing step to eliminate excessive material. Assays were carried out at 20 °C in buffer A (for protein binding), buffer B (for peptide binding), or PBS (for antibody binding). All buffers were supplemented with 0.5% gelatin, 3% gelatin hydrolysate, and 0.05% Tween 20 to avoid nonspecific binding. The interaction was monitored at 405 nm using alkaline phosphatase-labeled anti-Ig antibody (1/2000) and streptavidin (1/1000) for antibody testing and all other experiments, respectively. Control assays were carried out in wells saturated with gelatin and gelatin hydrolysate only. Each assay was conducted in triplicate, and the mean value was plotted after subtraction of the nonspecific absorption. The binding parameters [apparent dissociation constant K_d and the maximum binding (A_{max})] were determined by nonlinearly fitting

$$A = A_{max}[L]/(K_d + [L]) \quad (1)$$

where A is the absorbance at 405 nm and [L] is the ligand concentration by using the CURVE FIT software developed by K. Raner Software (Victoria, Australia). Additional details are given in the figure legends.

Fluorescence Measurements. Fluorescence experiments were conducted using an LS 50 Perkin-Elmer luminescence spectrometer. The intrinsic fluorescence of tryptophan was obtained in buffer B at 20 °C. The excitation wavelength was set at 280 nm, and emission spectra were recorded between 320 and 360 nm. Spectra for AEDANS-labeled monomeric actin or peptides, using buffer A or buffer B, respectively, were obtained with the excitation wavelength set at 340 nm and emission spectra recorded between 440 and 520 nm. Spectra for FITC-labeled plastin were obtained with the excitation wavelength set at 480 nm and emission spectra recorded between 500 and 550 nm. Fluorescence changes were deduced from the area of emission spectra. Mean values for at least four measurements were reported versus ligand concentrations. Parameters, apparent K_d and F_{max} (maximum fluorescence), were calculated in the same way as in the ELISA (eq 1), assuming a stoichiometry of 1. Depolymerization of pyrenyl F-actin was followed by a decrease in pyrene fluorescence (excitation at 365 nm and emission at 390 nm) after a quick dilution in depolymerizing buffer.

Cross-Linking Reactions. F-Actin (290 μg/mL) and plastin domains (actin/ABD molar ratio of 2/1 or 1/1) were incubated in buffer C supplemented with 2 mM $MgCl_2$. The complexes were cross-linked with 10 mM EDC/NHS, 1 mM EEDQ [*N*-(ethoxycarbonyl)-2-ethoxy-1,2-dihydroquinoline], or 0.01% glutaraldehyde (1 mM) as described previously (*36*). The reactions were allowed to proceed for 50 min (glutaraldehyde) or 60 min (EDC/NHS and EEDQ). The cross-linked species were separated by gel electrophoresis and further analyzed by immunodetection using both anti-plastin domains and anti-actin antibodies (*34*).

Analytical Methods. SDS−polyacrylamide gel electrophoresis (SDS−PAGE) was performed using a mini Protean II apparatus (Bio-Rad) on 10% gels as described by Laemmli (*37*). Protein concentrations were measured spectrophotometrically as described previously (*27*). ABD1 and ABD2 fragment concentrations were determined with extinction coefficients ($A_{280}^{0.1\%}$) of 0.82 and 1.3 and molecular masses of 30 and 28 kDa, respectively. Peptide solutions were quantified using amino acid analysis.

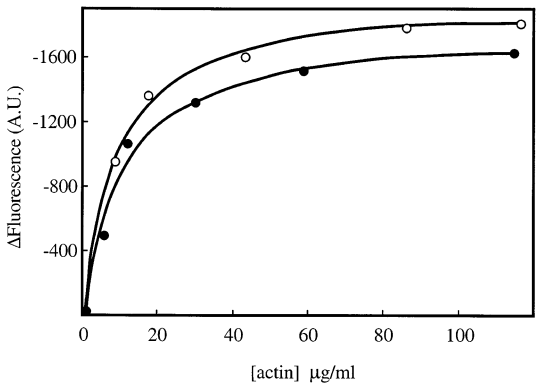

FIGURE 2: Interaction of L-plastin with F-actin from skeletal α-actin and cytoplasmic β-actin isoforms assessed using the fluorescence assay. The change in fluorescence emission (hypochromic effect) of FITC plastin (2.4 μg/mL) was recorded in the presence of increasing amounts (0−115 μg/mL) of skeletal muscle (○) and cytoplasmic (●) actin. The experiment was carried out in 100 mM KCl, 2 mM $MgCl_2$, 1 mM EGTA, and 20 mM Tris (pH 7.4). Fluorescence changes were calculated from the area of emission spectra and expressed in arbitrary units. Fitting of experimental data points was carried out as described in Experimental Procedures.

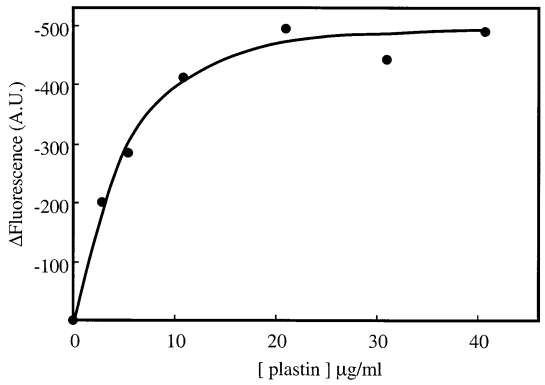

FIGURE 3: Interaction of L-plastin with monomeric actin assessed using fluorescence. The change in fluorescence emission of dansylated actin (0.24 μM) was observed at various plastin concentrations (0−0.6 μM) in buffer A. Fluorescence changes were calculated from the area of emission spectra and expressed in arbitrary units.

RESULTS

L-Plastin Binds F-Actin without Any Isoform Specificity. We have investigated the interaction of L-plastin with filamentous actin using both solid phase and solution experiments. Using fluorescence experiments, we have compared the binding of FITC plastin to increasing amounts of skeletal muscle and non-muscle actin. Results (Figure 2) show a saturable change in the fluorescence of the labeled plastin (hypochromic effect) with no significant difference in the apparent dissociation constants whatever the actin isoform (K_d = 0.26 ± 0.05 and 0.22 ± 0.02 μM for cytoplasmic and skeletal actin, respectively). This result was confirmed using solid phase and cosedimentation assays (not shown). For practical reasons, skeletal actin was then used for all other experiments.

Monomeric Actin−L-Plastin Interaction and Identification of Two Actin Sequences Involved in Plastin Binding. Using fluorescence experiments, we have tested the effect of increasing the amounts of plastin added to dansylated skeletal actin (10 μg/mL). We observed that the addition of plastin shows a fluorescence change (hypochromic effect) that saturates (Figure 3). This experiment shows that *in vitro* L-plastin interacts with G-actin which indicates that binding structures exist on a single actin molecule.

The second part of the study was carried out using four synthetic actin peptides, chosen for their participation in α-actinin, filamin, or dystrophin binding (*27*, *29*, *33*, *35*). To test whether these peptides are implicated in the binding, we performed ELISA and fluorescence experiments, using either unlabeled or labeled peptides.

Plastin intrinsic fluorescence was monitored in fluorescence experiments after addition of increasing amounts of peptides, taking advantage of the absence of tryptophan in sequences of residues 112−125 and 360−372. Plastin possesses eight tryptophan residues; the average emission fluorescence spectrum is centered near 340 nm, a sign of a rather hydrophobic environment when compared to the value of 360 nm obtained in solution. We observed that addition of each peptide was responsible for a decrease in the plastin

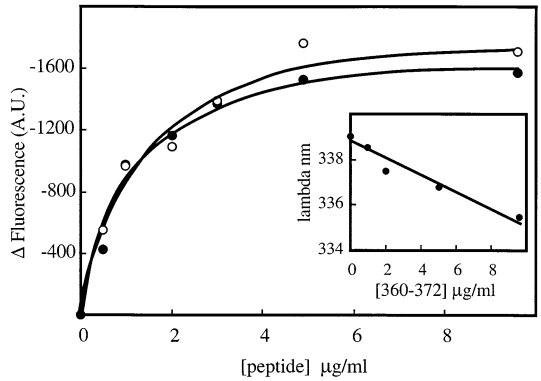

FIGURE 4: Interaction of plastin with actin peptides assessed using fluorescence. Changes in the plastin intrinsic fluorescence (12 μg/mL) were monitored in the presence of increasing amounts (0−9.6 μg/mL) of peptides 112−125 (●) and 360−372 (○) in buffer B. Fluorescence changes were calculated from the area of emission spectra and expressed in arbitrary units. Fitting of experimental data points was carried out as described in Experimental Procedures. The inset shows the decrease in the wavelength of the plastin maximum fluorescence associated with addition of peptide 360−372.

fluorescence emission (Figure 4). Further, the addition of peptide 360−372 was associated with a blue shift of 4 nm (Figure 4, inset). The binding curves obtained with the two peptides were shown to be nearly identical. The same saturable effect was obtained when we measured the change in the fluorescence of dansylated peptide 112−125 after plastin addition. However, no change was detected when dansylated peptide 360−372 was used. This apparent discrepancy may be due to the position of the label, located at the NH_2-terminal part of peptide 360−372, either too far to report the binding or right in the interaction site. Indeed, the longer dansylated peptide of residues 355−375, labeled at the COOH-terminal extremity (C374), binds plastin (not shown). The interaction of these peptides (including the dansylated ones) with plastin was further investigated using an ELISA. Apparent dissociation constants were calculated for peptides 112−125 and 360−372 and dansylated peptide 360−372: 0.75 ± 0.1, 0.3 ± 0.1, and 0.44 ± 0.1 μM, respectively. A negative control was created by the absence of binding of peptide 105−120, previously shown to interact with filamin (*35*).

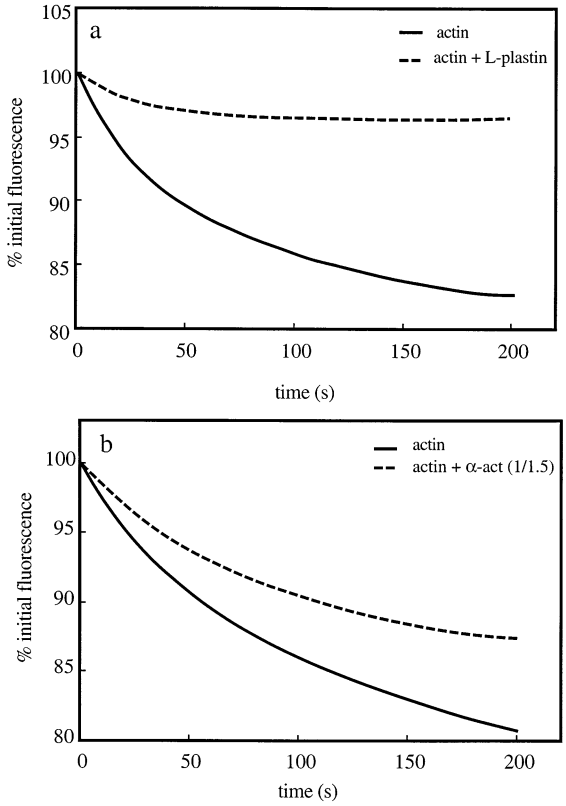

FIGURE 5: Actin cross-linking proteins inhibit microfilament depolymerization. (a) The depolymerization of pyrenyl actin was induced by a 10-fold dilution in depolymerizing buffer (buffer A) of the actin stock freshly prepared at 300 μg/mL (7.1 μM). The pyrenyl F-actin depolymerization alone (solid line) and in the presence of L-plastin (dashed line) were followed by losses in pyrene fluorescence during an initial period (from 0 to 200 s). Note that L-plastin was previously dialyzed against low-ionic strength buffer [10 mM KCl, 1 mM EGTA, and 10 mM MOPS (pH 7.1)]. Data are plotted as the percent fluorescence relative to the amount of fluorescence at time zero. (b) The same experiment was performed with α-actinin, using buffer G as the depolymerizing buffer.

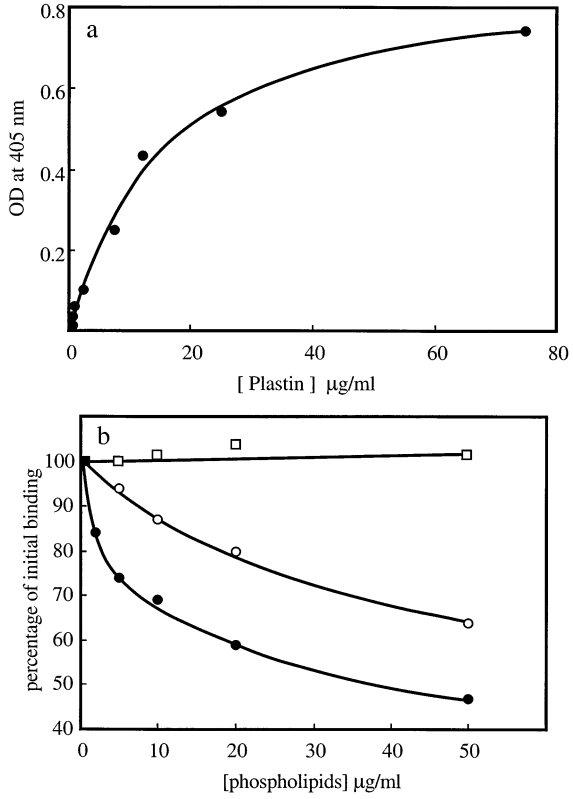

FIGURE 6: Effect of phosphoinositides on the monomeric actin−plastin interaction. (a) Increasing concentrations of biotinylated plastin (0−75 μg/mL) were allowed to interact with G-actin, coated under nonpolymerizing conditions (300 ng/mL). The interaction was monitored at 405 nm after incubation with alkaline phosphatase-labeled streptavidin (1/1000). Other details are found in Experimental Procedures. (b) Increasing concentrations of PIP2 (●), PI (○), and diacylglycerol (□) were preincubated with biotinylated plastin (10 μg/mL) and allowed to interact with immobilized monomeric actin (300 ng/mL). Note that PIP2, PI, and DAG were obtained as lyophilized powders and resuspended in distilled water; additionally, solutions were sonicated before they were used in assays. The binding of labeled plastin, expressed as a percentage of the initial binding, was monitored at 405 nm using alkaline phosphatase-labeled streptavidin (1/1000).

Depolymerization of Pyrenyl F-Actin Is Inhibited by Actin Cross-Linking Proteins. α-Actinin was previously reported to stabilize the microfilament as shown by the inhibition of the rate of pyrenyl F-actin depolymerization (*38*). The participation of the two actin sequences, namely, peptides 112−125 and 360−372, previously implicated in α-actinin binding (*27*, *29*) and their orientation (position) in the actin molecule led us to wonder about an eventual stabilization of the filament by lateral binding of L-plastin to two actin molecules. To test this hypothesis, we followed the depolymerization of pyrenyl actin induced by a quick 10-fold dilution of filamentous actin (300 μg/mL) in the absence or presence of L-plastin (actin/plastin molar ratio of 1/1). The result (Figure 5a) shows that L-plastin decreases the initial rate of actin depolymerization. This effect appeared to be even more important than the one observed with α-actinin (Figure 5B). This result can be attributed to the stabilization of the filaments by ABP, althought we cannot rule out the eventuality of a decrease in the critical concentration. Note that we have also investigated the effect of L-plastin on actin pyrene polymerization and did not find any significant modification of the polymerization process due to the presence of the ABP (not shown).

Effect of Phosphoinositides in the Regulation of the Plastin−Actin Interaction. The discovery of an increasing number of proteins whose interactions with actin are regulated by phosphoinositides, particularly in the α-actinin family, led us to evaluate the influence of such phospholipids on plastin−actin association. This was performed using solid phase immunoassays in which the binding of a constant amount of labeled plastin to immobilized monomeric actin was followed in the presence of increasing amounts of phospholipids (Figure 6). To set up this experiment, we have investigated L-plastin binding with G-actin using the same technique to determine the concentration of plastin to use for the competition assay. The result (Figure 6A) shows that plastin interacts with G-actin with an apparent dissociation constant of 0.25 ± 0.04 μM. The competition assay was then performed using 10 μg/mL L-plastin. We found (Figure 6B) that in the presence of PIP2, and to a smaller extent PI, the level of actin−L-plastin interaction decreased regularly. The observed inhibitory effect reaches 50% for 50 μg/mL PIP_2, a concentration generally used for dissociation of the actin−ABP complex (*39*). In contrast, diacylglycerol did not display such an effect.

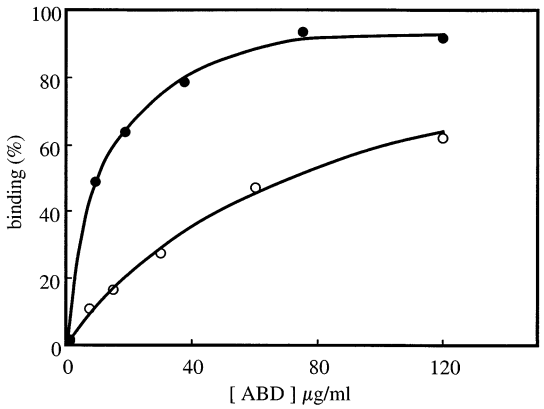

FIGURE 7: ABD1 and ABD2 display different affinities for actin. The binding of actin-binding domains was performed using an ELISA. Increasing concentrations (from 0 to 120 μg/mL) of ABD1 (●) or ABD2 (○), diluted in buffer C, were allowed to interact with coated F-actin. See Experimental Procedures for details. The binding of labeled ABDs (percentage) was calculated from the absorbance at 405 nm after addition of alkaline phosphatase-conjugated streptavidin (1/1000). Apparent dissociation constants were calculated to be 0.34 ± 0.04 and 2.6 ± 0.3 μM for ABD1 and ABD2, respectively.

As a result, the interaction of L-plastin with actin looks very similar to that of α-actinin. However, the presence of two actin-binding domains on the L-plastin molecule led us to further investigate the functionality and the equivalence of the two ABDs.

Functionality and Difference in the Way the Two ABDs Interact with Actin. The functional aspect was investigated using solid phase and solution experiments performed with recombinant domains (Figure 1b). Using an ELISA, we observed that both isolated domains were able to interact with immobilized actin (Figure 7) and that ABD1 binds actin with a higher affinity than does ABD2. The same result was observed for both F- and G-actin (not shown). Single domains were shown to bind actin peptides 112−125 and 360−372 without a significant difference (not shown).

The difference in the way the two ABDs bind actin was further investigated using cross-linking experiments followed by gel electrophoresis analysis associated with immunodetection (Figure 8). For this purpose, we tested three different reagents, two zero-length cross-linkers, 1-ethyl-3-[3-(dimethylamino)propyl]carbodiimide (EDC), the hydrophobic *N*-(ethoxycarbonyl)-2-ethoxy-1,2-dihydroquinoline (EEDQ), and glutaraldehyde. Using ABD2, we found that EDC was able to generate a major covalent product with an apparent molecular mass of 67 kDa with actin (Figure 8a). The double reactivity of this product with the anti-ABD2 and anti-actin antibodies (Figure 8b) associated with its molecular mass suggests that it likely corresponds to a 1/1 complex. The EEDQ or glutaraldehyde treatment yielded the same product in a minor quantity (not shown). Under the same conditions, no detectable covalent products were obtained with ABD1 (Figure 8A), whatever the cross-linker reagent. The different behavior of these cross-linker reagents demonstrates that ABD1 and ABD2 are highly susceptible to displaying different interfaces with actin.

We tested the effect of the two isolated domains on the initial rate of actin depolymerization. Using conditons identical to those used with the whole plastin molecule, we observed that ABD1 strongly reduces the initial rate of actin depolymerization (Figure 9a). On the other hand, the presence of ABD2 was responsible for an immediate and complete quenching of the fluorescence emission of pyrenyl actin (probably due to conformational changes in the actin molecule), impeding any interpretation concerning an eventual role of this domain in the initial rate of actin depolymerization. Using depolymerizing conditions, sedimentation of filamentous actin in the presence of each domain finally allowed us to investigate the role of ABD2 in microfilament stability. Indeed, after incubation of actin alone for 24 h, actin with ABD1, and actin with ABD2 under depolymerizing conditions and ultracentrifugation at 300000*g*, we observed (Figure 9b) that 87% of the actin remains in the pellet in the presence of ABD2 as compared to 22% obtained with ABD1 and 4% with actin alone. This result indicates that both domains protect actin from depolymerization, though ABD2 appears to be more efficient than ABD1 in this role.

DISCUSSION

This study was undertaken in an effort to better understand the L-plastin−actin interaction. Indeed, the very low yield of the plastin preparation has first hampered detailed biochemical characterization of the L-plastin−actin interaction (*17*, *18*). With the development of molecular tools, a recombinant protein has often been used to overcome the low yield of the fimbrin preparation. In the case of L-plastin,

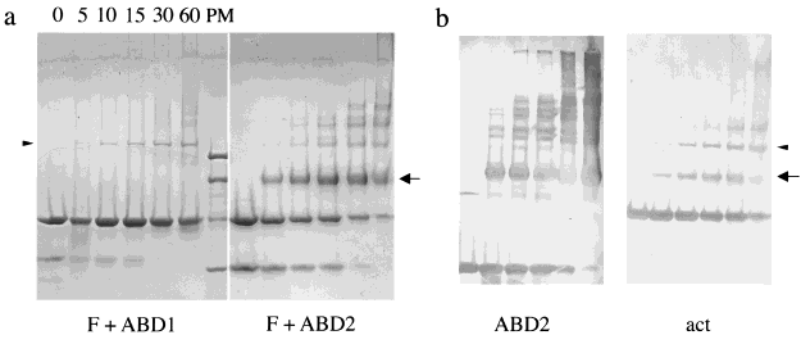

FIGURE 8: Cross-linking patterns of ABDs with EDC/NHS. The cross-linking reactions (after 0, 5, 10, 15, 30, and 60 min) were carried out as specified in Experimental Procedures. SDS−PAGE was performed on a 10% acrylamide gel and then stained with Coomassie blue (a). Molecular mass markers are indicated (97, 66, 45, and 33 kDa). Identification of ABD2 (ABD2) and actin (act) in the EDC/NHS-cross-linked products after immunodetection using anti-ABD2 (0.5 μg/mL) and anti-actin (2 μg/mL) antibodies, respectively (b). Actin polymer species (115 kDa) are denoted with arrowheads, and the major actin−ABD2 cross-linked product is denoted with an arrow. Note that, when loaded at equivalent concentrations, ABD1 staining with Coomassie blue is fainter than that observed with ABD2.

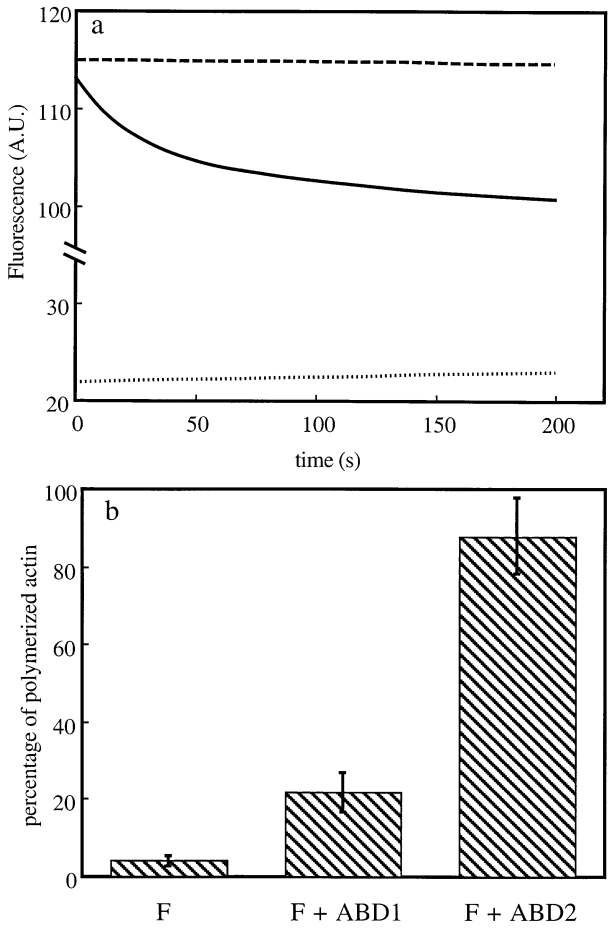

FIGURE 9: Influence of actin-binding domains on actin depolymerization induced by rapid dilution. In panel a, the initial rate of pyrenyl F-actin depolymerization was monitored using an experimental procedure similar to that described in the legend of Figure 5. Filamentous actin, diluted 10-fold in buffer G, was allowed to depolymerize alone (solid line), with ABD1 (dashed line), or with ABD2 (dotted line). Both domains (previously dialyzed against low-ionic strength buffer) were used at an actin/ABD molar ratio of 1/1. (b) F-Actin content was assayed after incubation for 24 h by high-speed centrifugation. Filamentous actin alone (0.7 μM, lane F), actin with 0.7 μM ABD1 (F + ABD1), or actin with 0.7 μM ABD2 (F + ABD2) was incubated in buffer G for 24 h at 4 °C, and then sedimented for 30 min at 300000*g* using a TL120 ultracentrifuge. The supernatants and pellets were separated by SDS−PAGE (12.5%). The gel was scanned, and the amount of polymerized actin was calculated using a known actin amount as a control. The experiment was repeated ($n = 4$). Shown in the figure is the percentage of polymerized actin (±standard deviation) present under each condition, in a representative experiment.

the actin bundling activity of the recombinant ABP was validated using electron microscopy (*32*). The work presented here illustrates the similitudes that exist between L-plastin and α-actinin's interfaces with actin, and for the first time demonstrates using biochemical techniques that both actin-binding domains (ABDs) of the molecule are functional and nonequivalent in terms of affinity and interfaces toward actin.

The plastin−actin interaction was not found to be sensitive to the actin isoform as demonstrated by the use of two different α-skeletal and cytoplasmic actin isoforms in solid phase assays and cosedimentation assays (not shown). This finding is consistent with the participation of the two highly conserved sequences, namely, peptides 112−125 and 360−372, in the binding (only one amino acid change at position 365 between the skeletal α-actin and cytoplasmic β-actin isoforms). In agreement with the implication of actin residues 112−125 is the fact that mutation of amino acid 120 abolishes plastin binding (*40*). The notion of highly conserved interfaces was previously noted by Honts and coworkers in their study of yeast suppressor mutations (*41*). The residues presented as the most susceptible to forming a binding surface by structural analysis (*25*) are also highly conserved between skeletal α-actin and cytoplasmic β-actin with the exception of one residue in the NH_2-terminal part (Thr6), which strengthens the idea of conserved interfaces for binding of both actin isoforms to L-plastin. Taken together, these results contrast with the finding that only cytoplasmic β-actin would bind L-plastin (*17*). We should mention that skeletal α-actin has been reported to interact with chicken fimbrin (*42*), the human T-plastin (*24*), and more recently *Tetrahymena pyriformis* fimbrin (*43*) and AtFim1 from *A. thaliana* (*44*).

The concept of lateral binding concerning this family of proteins appeared as a result of a molecular modeling experiment performed on a complex of the α-actinin actin-binding domain and filamentous actin (*45*). Then, Hanein *et al*. (*25*) proposed a model in which the first 375 amino acids of fimbrin (T-plastin) interacted with F-actin, and finally, Volkmann *et al*. (*26*) recently generated an atomic model of the complete fimbin−actin−actin cross-link. In all these studies, the ABP interacts between two actin monomers. It is important to mention here that the molecular modeling approach combines information from biochemical data, atomic coordinates, and density maps from electron cryomicroscopy. This strengthens the necessity of integrating knowledge from both origins. The notion of lateral binding is in agreement with the protection brought by L-plastin against depolymerization of the microfilament. The idea of stabilization of the filament (without a direct demonstration) was introduced by Karpova *et al*. (*40*), confirmed by Belmont *et al*. (*46*), and further supported by Cheng *et al*. (*47*), all working on yeast. More recently, the notion of protection against microfilament depolymerization induced by profilin was demonstrated with *A. thaliana* fimbrin (*44*). In our case, the result of protection against depolymerization was observed in both short and long experiments, using L-plastin and further confirmed with isolated domains. We should mention that plastin/fimbrins are not the only bundling proteins to protect filaments from disassembly since a protein from *Dictyostelium* (30 kDa) was found to have the same role (*48*).

We have identified two sequences of actin subdomain 1 involved in plastin binding, namely, peptides 112−125 (a complete helical region in the actin structure) and 360−372, that are consistent with the concept of lateral binding. Circular dichroism measurements have revealed a strong propensity for adopting helical structure in the case of peptide 112−125 (*49*), whereas peptide 360−372 appeared to be randomly structured. Since α-actinin was found to interact with the same sequences (*27*, *29*), the plastin−actin interface could resemble that of α-actinin and actin, in agreement with previous speculation (*24*, *50*). This conclusion is confirmed by the absence of binding of both plastin and α-actinin to peptide 105−120, which interacts with filamin (*27*, *35*). Additional interactions on the actin surface, such as amino acids 99 and 100, may allow specific recognition of plastin

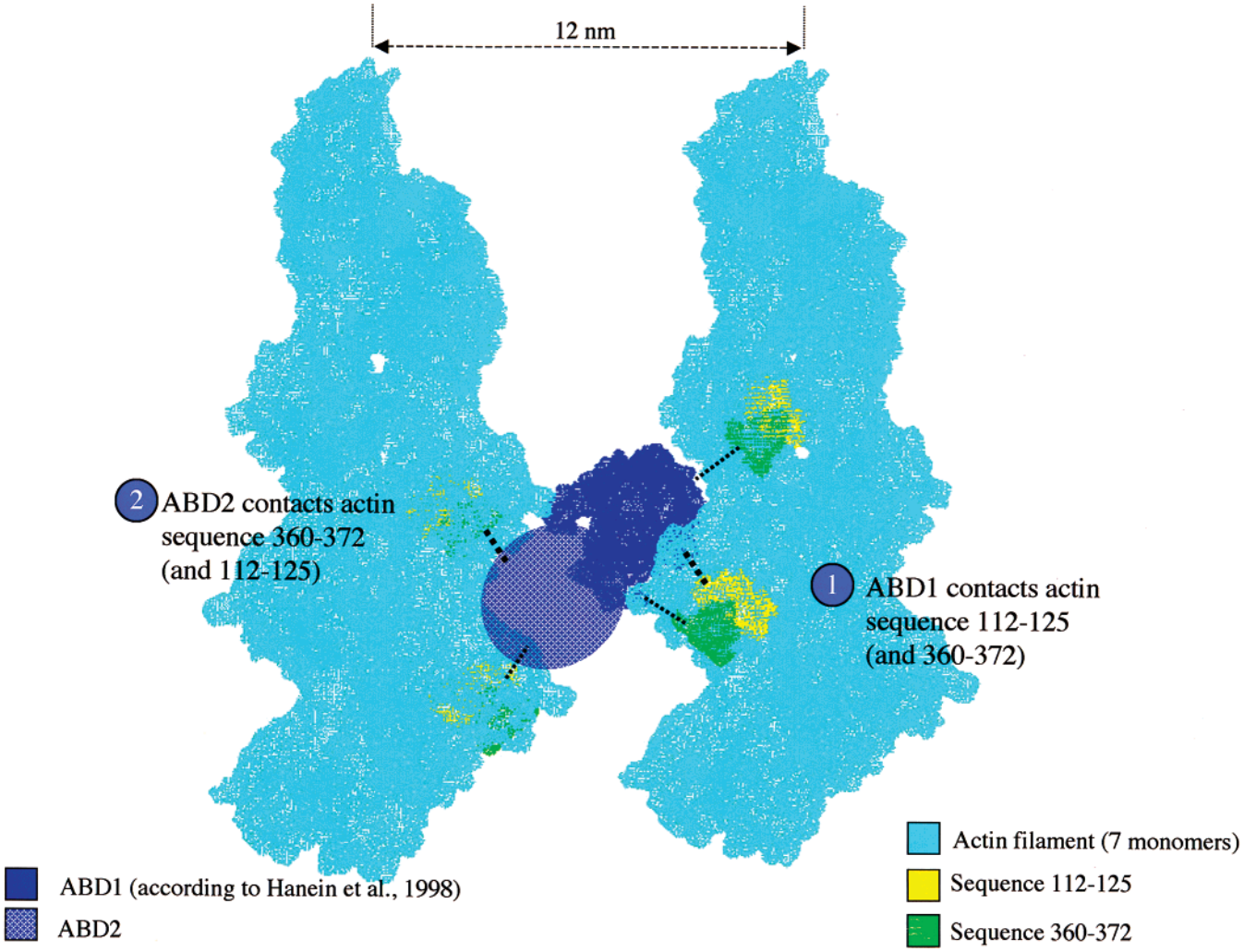

FIGURE 10: Summary of the plastin−actin contacts on the actin filament. The atomic model of F-actin (seven monomers) was borrowed from Lorenz *et al*. (*58*). The spatial relationship between the filaments and ABD1 was taken from the atomic model of the actin−ABD1 complex and kindly provided by Hanein *et al*. (*25*). The positioning of the second actin filament (left side of the figure) was obtained by a translatory movement of 12 nm, keeping the filaments in register, as demonstrated by Volkmann *et al*. (*26*). The spatial relationship between the filaments and ABD2 (drawn as a sphere equal in size to ABD1) was also taken from the proposed model of Volkmann *et al*. (*26*). Contacts between actin sequences identified in this study (colored yellow and green, for peptides 112−125 and 360−372, respectively) and the two actin-binding domains are depicted with dashed lines, thick or narrow according to the relative importance of the contact. Note that in this model, the contact zone(s) of the ABD2 appears at the back of the actin filament (left side). The sequence of events would be as follows: (1) the interaction of ABD1 with actin residues 112−125 and probably residues 360−372 after a conformational change in the COOH-terminal region of actin upon ABD1 binding (*24*) (not visible in this model) and (2) ABD2 contacting actin residues 360−372 and probably residues 112−125 on the neighboring filament. Note that the movement on subdomain 1 of actin upon ABD1 binding would decrease the distance (8−9 Å) between actin and the actin-binding domain and make possible the contact. The figure, showing molecular surfaces, was generated using Swiss Pdb Viewer.

(*41*). Note that the molecular model of Hanein and co-workers proposes the participation of other segments of the actin molecule, in particular, amino acids 21−28 and 41 (*25*), while a similar approach applied to the α-actinin−actin interface identifies only two zones of interaction, namely, peptides 86−117 and 350−375 (*45*).

We have observed an inhibitory effect of phosphoinositides (~50% inhibition with PIP2) on the interaction between G-actin and L-plastin. This experiment introduces the notion of G-actin binding for a bundling protein and questions about the rather high apparent dissociation constant that was found. In fact, plastin is not the only bundling protein that is able to interact with G-actin, since similar capacities were found for ABP50 from *Dictyostelium* and α-actinin (*29*, *51*, *52*). In the latter case, calculated apparent dissociation constants for both G- and F-actin were found in the same range (0.3−0.4 μM) (*52*, *53*). We have used this capacity for *in vitro* interaction in this experiment to facilitate the interpretation. With regard to the observed effect of phosphoinositides, it is very similar to what was previously observed for α-actinin (*54*), filamin (*55*), and dystrophin (*56*). PIP2 binding sites were proposed on the surface of the ABP (*56*). Our observation strengthens the idea of a protein family with sequence similarity, which interacts with overlapping interfaces on actin and also shares a common regulation mechanism.

The functionality and the equivalence of the two actin-binding domains were investigated in an effort to better understand the mechanism of binding of plastin to actin. As a result, both isolated domains were shown to be functional, with ABD1 having a significantly higher affinity for actin than ABD2. Interestingly, both domains seem to have

different interfaces with actin as revealed by cross-linking experiments and protection against microfilament depolymerization. The different mode of interfacing with the actin filament for the two ABDs was previously proposed (*23*, *26*, *44*, *57*). The distinction made here between the two domains can be explained by a careful analysis of the primary sequence. Indeed, ABD1 and ABD2 from the same isoform are less similar (22% identical in the case of L-plastin) than two ABD1 sequences from different sources (L- and T-isoforms being 82% identical); in particular, ABD1 possesses a linker sequence between its two CH domains which is much longer than in ABD2 (see Figure 4 in ref *26*).

Finally, the analysis of our results in light of the recent modeling work (*26*) allows a better understanding of the mechanism of assembly between plastin and actin, built on the current model (see Figure 10). In this mechanism, we propose that ABD1 would bind first to actin. This is due to an observation from a depolymerization experiment in which ABD1 and the whole molecule give similar results compared to the total quenching observed in the presence of ABD2. This is strengthened by the higher affinity of ABD1 for actin than that of ABD2. The binding of ABD1 of one fimbrin molecule would in turn induce a conformational change in actin, which favors binding of ABD2 of another fimbrin molecule (eventual increase in affinity) which would cancel the observed quenching in the fluorescence signal. Such conformational change was proposed in subdomain 1 upon binding of fimbrin fragment 1−375 (*24*). However, we cannot rule out the possibility that the data observed with the whole molecule are due to an exclusive binding of ABD1, resulting in binding and not cross-linking. The most favorable contact zone for ABD1 on actin structure would certainly be peptide 112−125 and amino acids in the exposed loop of residues 90−100 (*25*). The participation of actin residues 360−372 in the direct interaction with the fimbrin actin-binding domains appears to be incompatible with the current structural model (*25*). Indeed, the actual distance between these actin residues and fimbrin would be too large for direct interaction by 8−9 Å even if all uncertainties are taken into account (D. Hanein, personal communication). However, this discrepancy could be explained by a movement of the COOH-terminal region of actin induced by fimbrin binding, as shown by Hanein *et al*. (*24*). We also propose that ABD2 establishes a strong contact with the COOH terminus of the actin sequence as revealed by the nature of the quenching in the fluorescence emission observed upon binding of ABD2 to filamentous actin labeled on Cys374 either with pyrene (Figure 9a) or with dansyl (not shown). One should keep in mind that the stabilization against actin depolymerization observed with each domain implies a localization between two monomers and thus more than a single contact on the actin molecule. This would explain why we were not able to distinguish ABD1 and ABD2 in their binding to actin peptides.

It is now clear that ABD1 and ABD2 of L-plastin are functionally different as far as actin binding is concerned. The difference is further supported by the discovery of a vimentin binding site in the first CH domain of ABD1 (*6*). Would the future bring some new binding partners and/or strenghten the difference between the two actin-binding domains?

ACKNOWLEDGMENT

We thank Dr. D. Louvard's group for providing the pGEX 2T construct with L-plastin. Moreover, we are very grateful to Dr. Niels Hanein for providing the actin−ABD1 coordinates and to Dr. Dorit Hanein for constructive discussions concerning the atomic model.

REFERENCES

1. de Arruda, M. V., Watson, S., Lin, C. S., Leavitt, J., and Matsudaira, P. (1990) Fimbrin is a homologue of the cytoplasmic phosphoprotein plastin and has domains homologous with calmodulin and actin gelation proteins, *J. Cell Biol. 111*, 1069−1079.
2. Adams, A. E., Shen, W., Lin, C. S., Leavitt, J., and Matsudaira, P. (1995) Isoform-specific complementation of the yeast sac6 null mutation by human fimbrin, *Mol. Cell. Biol. 15*, 69−75.
3. Bretscher, A. (1981) Fimbrin is a cytoskeleton protein that crosslinks F-actin in vitro, *Proc. Natl. Acad. Sci. U.S.A. 78*, 6849−6853.
4. Daudet, N., and Lebart, M.-C. (2002) Transient expression of the T-isoform of plastin/fimbrin in the stereocilia of developing auditory hair cells, *Cell Motil. Cytoskeleton 53*, 326−336.
5. Hofer, D., and Drenckhahn, D. (1996) Cytoskeletal differences between stereocilia of the human sperm passageway and microvilli/stereocilia in other locations, *Anat. Rec. 245*, 57−64.
6. Correia, I., Chu, D., Chou, Y.-H., Goldman, R. D., and Matsudaira, P. (1999) Integrating the actin and vimentin cytoskeletons: adhesion-dependent formation of fimbrin-vimentin complexes in macrophages, *J. Cell Biol. 146*, 831−842.
7. Lin, C. S., Aebersold, R. H., and Leavitt, J. (1990) Correction of the N-terminal sequences of the human plastin isoforms by using anchored polymerase chain reaction: identification of a potential calcium-binding domain, *Mol. Cell. Biol. 10*, 1818−1821.
8. Zu, Y. L., Shigesada, K., Nishida, E., Kubota, I., Kohno, M., Hanaoka, M., and Namba, Y. (1990) 65-kilodalton protein phosphorylated by interleukin 2 stimulation bears two putative actin-binding sites and two calcium-binding sites, *Biochemistry 29*, 8319−8324.
9. Shinomiya, H., Hagi, A., Fukuzumi, M., Mizobuchi, M., Hirata, H., and Utsumi, S. (1995) Complete primary structure and phosphorylation site of the 65-kDa macrophage protein phosphorylated by stimulation with bacterial lipopolysaccharide, *J. Immunol. 154*, 3471−3478.
10. Lin, C. S., Lau, A., and Lue, T. F. (1998) Analysis and mapping of plastin phosphorylation, *DNA Cell Biol. 17*, 1041−1046.
11. Watanabe, A., Yonemura, I., Gonda, K., and Numata, O. (2000) Cloning and sequencing of the gene for a *Tetrahymena* fimbrin-like protein, *J. Biochem. 127*, 85−94.
12. McCurdy, D. W., and Kim, M. (1998) Molecular cloning of a novel fimbrin-like cDNA from *Arabidopsis thaliana*, *Plant Mol. Biol. 36*, 23−31.
13. Lin, C. S., Park, T., Chen, Z. P., and Leavitt, J. (1993) Human plastin genes. Comparative gene structure, chromosome location, and differential expression in normal and neoplastic cells, *J. Biol. Chem. 268*, 2781−2792.
14. Zheng, J., Rudra-Ganguly, N., Miller, G. J., Moffatt, K. A., Cote, R. J., and Roy-Burman, P. (1997) Steroid hormone induction and expression patterns of L-plastin in normal and carcinomatous prostate tissues, *Am. J. Pathol. 150*, 2009−2018.
15. Chung, I., Schwartz, P. E., Crystak, R. G., Pizzorno, G., Leavitt, J., and Deisseroth, A. B. (1999) Use of L-plastin promotor to develop an adenoviral system that confers transgene expression in ovarian cancer cells but not in normal mesothelial cells, *Cancer Gene Ther. 6*, 99−106.
16. Zheng, J., Rudra-Ganguly, N., Powell, W. C., and Roy-Burman, P. (1999) Suppression of prostate carcinoma cell invasion by expression of antisense L-plastin gene, *Am. J. Pathol. 155*, 115−122.
17. Namba, Y., Ito, M., Zu, Y., Shigesada, K., and Maruyama, K. (1992) Human T cell L-plastin bundles actin filaments in a calcium-dependent manner, *J. Biochem. 112*, 503−507.
18. Pacaud, M., and Derancourt, J. (1993) Purification and further characterization of macrophage 70-kDa protein, a calcium-regulated, actin-binding protein identical to L-plastin, *Biochemistry 32*, 3448−3455.

19. Goldsmith, S. C., Pokala, N., Shen, W., Fedorov, A. A., Matsudaira, P., and Almo, S. C. (1997) The structure of an actin-crosslinking domain from human fimbrin, *Nat. Struct. Biol. 4*, 708−712.
20. Carugo, K. D., Banuelos, S., and Saraste, M. (1997) Crystal structure of a calponin homology domain, *Nat. Struct. Biol. 4*, 175−179.
21. Keep, N. H., Norwood, F. L., Moores, C. A., Winder, S. J., and Kendrick-Jones, J. (1999) The 2.0 Å structure of the second calponin homology domain from the actin-binding region of the dystrophin homologue utrophin, *J. Mol. Biol. 285*, 1257−1264.
22. Keep, N. H., Winder, S. J., Moores, C. A., Walke, S., Norwood, F. L., and Kendrick-Jones, J. (1999) Crystal structure of the actin-binding region of utrophin reveals a head-to-tail dimer, *Struct. Folding Des. 7*, 1539−1546.
23. Gimona, M., Djinovic-Carugo, K., Kranewitter, W. J., and Winder, S. J. (2002) Functional plasticity of CH domains, *FEBS Lett. 513*, 98−106.
24. Hanein, D., Matsudaira, P., and DeRosier, D. J. (1997) Evidence for a conformational change in actin induced by fimbrin (N375) binding, *J. Cell Biol. 139*, 387−396.
25. Hanein, D., Volkmann, N., Goldsmith, S., Michon, A. M., Lehman, W., Craig, R., DeRosier, D., Almo, S., and Matsudaira, P. (1998) An atomic model of fimbrin binding to F-actin and its implications for filament crosslinking and regulation, *Nat. Struct. Biol. 5*, 787−792.
26. Volkmann, N., DeRosier, D., Matsudaira, P., and Hanein, D. (2001) An atomic model of actin filaments cross-linked by fimbrin and its implications for bundle assembly and function, *J. Cell Biol. 153*, 947−956.
27. Lebart, M. C., Méjean, C., Roustan, C., and Benyamin, Y. (1993) Further characterization of the α-actinin-actin interface and comparison with filamin-binding sites on actin, *J. Biol. Chem. 268*, 5642−5648.
28. Spudich, J. A., and Watt, S. (1971) The regulation of rabbit skeletal muscle contraction. I. Biochemical studies of the interaction of the tropomyosin-troponin complex with actin and the proteolytic fragments of myosin, *J. Biol. Chem. 246*, 4866−4871.
29. Lebart, M. C., Méjean, C., Roustan, C., and Benyamin, Y. (1990) Characterization of a new α-actinin binding site in the COOH-terminal part of the actin molecule, *Biochem. Biophys. Res. Commun. 173*, 120−126.
30. Takashi, R. (1979) Fluorescence energy transfer between subfragment-1 and actin points in the rigor complex of actosubfragment-1, *Biochemistry 18*, 5164−5169.
31. Kouyama, T., and Mihashi, K. (1981) Fluorimetry study of N-(1-pyrenyl)iodoacetamide-labelled F-actin. Local structural change of actin protomer both on polymerization and on binding of heavy meromyosin, *Eur. J. Biochem. 114*, 33−38.
32. Arpin, M., Friederich, E., Algrain, M., Vernel, F., and Louvard, D. (1994) Functional differences between L- and T-plastin isoforms, *J. Cell Biol. 127*, 1995−2008.
33. Lebart, M. C., Casanova, D., and Benyamin, Y. (1995) Actin interaction with purified dystrophin from electric organ of *Torpedo marmorata*: possible resemblance with filamin-actin interface, *J. Muscle Res. Cell Motil. 16*, 543−552.
34. Benyamin, Y., Roustan, C., and Boyer, M. (1986) Anti-actin antibodies. Chemical modification allows the selective production of antibodies to the N-terminal region, *J. Immunol. Methods 86*, 21−29.
35. Méjean, C., Lebart, M. C., Boyer, M., Roustan, C., and Benyamin, Y. (1992) Localization and identification of actin structures involved in the filamin-actin interaction, *Eur. J. Biochem. 209*, 555−562.
36. Bertrand, R., Chaussepied, P., and Kassab, R. (1988) Cross-linking of the skeletal myosin subfragment 1 heavy chain to the N-terminal actin segment of residues 40−113, *Biochemistry 27*, 5728−5736.
37. Laemmli, U. K. (1970) Cleavage of structural proteins during the assembly of the head of bacteriophage T4, *Nature 227*, 680−685.
38. Cano, M. L., Cassimeris, L., Fechleimer, M., and Zigmond, S. H. (1992) Mechanisms responsible for F-actin stabilization after lysis of polymorphonuclear leukocytes, *J. Cell Biol. 116*, 1123−1134.
39. Méjean, C., Lebart, M. C., Roustan, C., and Benyamin, Y. (1995) Inhibition of actin-dystrophin interaction by inositide phosphate, *Biochem. Biophys. Res. Commun. 210*, 152−158.
40. Karpova, T. S., Tatchell, K., and Cooper, J. A. (1995) Actin filaments in yeast are unstable in the absence of capping protein or fimbrin, *J. Cell Biol. 131*, 1483−1493.
41. Honts, J. E., Sandrock, T. S., Brower, S. M., O'Dell, J. L., and Adams, A. E. (1994) Actin mutations that show suppression with fimbrin mutations identify a likely fimbrin-binding site on actin, *J. Cell Biol. 126*, 413−422.
42. Glenney, J. R. J., Kaulfus, P., Matsudaira, P., and Weber, K. (1981) F-actin binding and bundling properties of fimbrin, a major cytoskeletal protein of microvillus core filaments, *J. Biol. Chem. 256*, 9283−9288.
43. Watanabe, A., Kurasawa, Y., Watanabe, Y., and Numata, O. (1998) A new *Tetrahymena* actin-binding protein is localized in the division furrow, *J. Biochem. 123*, 607−613.
44. Kovar, D. R., Staiger, C. J., Weaver, E. A., and McCurdy, D. W. (2000) AtFim1 is an actin filament crosslinking protein from *Arabidopsis thaliana*, *Plant J. 24*, 625−636.
45. McGough, A., Way, M., and Derosier, D. (1994) Determination of the α-actinin-binding site on actin filaments by cryoelectron microscopy and image analysis, *J. Cell Biol. 126*, 433−443.
46. Belmont, L. D., and Drubin, D. G. (1998) The yeast V159N actin mutant reveals roles for actin dynamics in vivo, *J. Cell Biol. 142*, 1289−1299.
47. Cheng, D., Marner, J., and Rubenstein, P. A. (1999) Interaction in vivo and in vitro between the yeast fimbrin, SAC6P, and a polymerization-defective yeast actin (V266G and L267G), *J. Biol. Chem. 274*, 35873−35880.
48. Zigmond, S. H., Furukawa, R., and Fechheimer, M. (1992) Inhibition of actin filament depolymerization by the *Dictyostelium* 30,000-Da actin-bundling protein, *J. Cell Biol. 119*, 559−567.
49. Renoult, C., Ternent, D., Maciver, S. K., Fattoum, A., Astier, C., Benyamin, Y., and Roustan, C. (1999) The identification of a second cofilin binding site on actin suggests a novel, intercalated arrangement of F-actin binding, *J. Biol. Chem. 274*, 28893−28899.
50. Matsudaira, P. (1994) The fimbrin and α-actinin footprint on actin, *J. Cell Biol. 126*, 285−287.
51. Yang, F., Demma, M., Warren, V., Dharmawardhane, S., and Condeelis, J. (1990) Identification of an actin-binding protein from *Dictyostelium* as elongation factor 1a, *Nature 347*, 494−496.
52. Papa, I., Mejean, C., Lebart, M. C., Astier, C., Roustan, C., Benyamin, Y., Alvarez, C., Verrez-Bagnis, V., and Fleurence, J. (1995) Isolation and properties of white skeletal muscle α-actinin from sea-trout (*Salmo trutta*) and bass (*Dicentrarchus labrax*), *Comp. Biochem. Physiol., Part B: Biochem. Mol. Biol. 112*, 271−282.
53. Meyer, R. K., and Aebi, U. (1990) Bundling of actin filaments by α-actinin depends on its molecular length, *J. Cell Biol. 110*, 2013−2024.
54. Fukami, K., Furuhashi, K., Inagaki, M., Endo, T., Hatano, S., and Takenawa, T. (1992) Requirement of phosphatidylinositol 4,5-bisphosphate for α-actinin function, *Nature 359*, 150−152.
55. Furuhashi, K., Inagaki, M., Hatano, S., Fukami, K., and Takenawa, T. (1992) Inositol phospholipid-induced suppression of F-actin-gelating activity of smooth muscle filamin, *Biochem. Biophys. Res. Commun. 184*, 1261−1265.
56. Méjean, C., Lebart, M. C., Roustan, C., and Benyamin, Y. (1995) Inhibition of actin-dystrophin interaction by inositide phosphate, *Biochem. Biophys. Res. Commun. 210*, 152−158.
57. Brower, S. M., Honts, J. E., and Adams, A. E. (1995) Genetic analysis of the fimbrin-actin binding interaction in *Saccharomyces cerevisiae*, *Genetics 140*, 91−101.
58. Lorenz, M., Popp, D., and Holmes, K. C. (1993) Refinement of the F-actin model against X-ray fiber diffraction data by the use of a directed mutation algorithm, *J. Mol. Biol. 234*, 826−836.

BI030151P